Syntheses and Molecular Structures of Liquid Pyrophoric Hydridosilanes

Maik Gerwig,[a] Uwe Böhme,*[a] Mike Friebel,[a] Franziska Gründler,[a] Georg Franze,[a] Marco Rosenkranz,[b] Horst Schmidt,[a] and Edwin Kroke[a]

Dedicated to Professor *Karl-Heinz Thiele* on the occasion of his 90th birthday.

Trisilane, isotetrasilane, neopentasilane, and cyclohexasilane have been prepared in gram scale. In-situ cryo crystallization of these pyrophoric liquids in sealed capillaries on the diffractometer allows access to the single crystal structures of these compounds. Structural parameters are discussed and compared to gas-phase electron diffraction structures from literature and with the results from quantum chemical calculations. Significantly higher packing indices are found for the silanes compared to the corresponding alkanes. Radiation with ultraviolet light (365 nm) and parallel ESR (EPR) measurement shows that cyclohexasilane is easily split into radicals, which subsequently leads to the formation of branched and chain-like oligomers. The other compounds form no radicals under these conditions. NMR spectra of all four compounds have been recorded.

1. Introduction

Hydridosilanes are linear, branched or cyclic compounds that consist only of silicon and hydrogen.[1] Monosilane (SiH_4), the smallest compound in this homologous series, is produced in an industrial scale as a precursor to produce elemental silicon for different applications.[2,3] The higher homologues of these compounds are seldom used, since they are difficult to handle and pyrophoric. However, the chemistry of hydridosilanes has received a considerable revival in recent years due to their potential use as precursors for liquid phase deposition of silicon films.[4–16] This approach promises significant reduction of processing costs in the manufacture of semiconductor devices.[4,17,18,19] Printing techniques have been applied to produce silicon thin-film transistors (TFT).[4,16,20] The production of other devices like light-emitting diodes,[17,19] large area flexible solar cells,[21] or ultrafine silicon patterns (10 nm or less)[22] have been forebode on the basis of this new technology.

Oligosilanes themselves are known for many years. Great efforts have been made to prepare and utilize these compounds. Pioneering work was performed by Stock and Somiesky since 1916. They prepared linear hydridosilanes Si_nH_{2n+2} up to hexasilane.[23–26] Their synthesis involved the hydrolysis of magnesium silicide. Thereby, a mixture of hydridosilanes is formed and subsequently separated by high vacuum distillation, following the so-called Stock-procedure.[27] Later, the work on hydridosilanes was continued by Fehér et al.[28] They published numerous papers on hydridosilanes including physicochemical and spectroscopic characterization.[29–34] The potential of energy-rich silicon hydrides for chemical propulsion of aircraft vehicles has been investigated by Hidding and others.[35,36]

Although hydridosilanes are known for more than one hundred fifty years[37] only very few crystal structures of such compounds have been published.[19,38] Herein we report the syntheses and molecular structures of selected linear, branched and cyclic hydridosilanes.

2. Results and Discussion

2.1. Chlorosilanes as Precursors

Chlorosilanes are versatile building blocks for the preparation of numerous silicon compounds.[39–44] Highly pure hexachlorodisilane is prepared in an industrial scale.[45,46] It is used for gas phase epitaxy of silicon at low temperatures.[2] Commercial samples of hexachlorodisilane, Si_2Cl_6 (**1**), octachlorotrisilane, Si_3Cl_8 (**2**), and perhalogenated isotetrasilane $ClSi(SiCl_3)_3$ (**3**), were utilized as starting materials for the preparation of the hydridosilanes investigated in this study.

The disproportionation of hexachlorodisilane and other chlorosilanes in presence of amines leads to perchlorinated oligosilanes. These reactions are known for more than sixty

[a] *M. Gerwig, Dr. U. Böhme, M. Friebel, F. Gründler, G. Franze, Dr. H. Schmidt, Prof. Dr. E. Kroke*
Institut für Anorganische Chemie
TU Bergakademie Freiberg
Leipziger Straße 29
09599 Freiberg (Germany)
E-mail: Uwe.Boehme@chemie.tu-freiberg.de
[b] *M. Rosenkranz*
Leibniz-Institut für Festkörper- und Werkstoffforschung Dresden
Helmholtzstraße 20
01069 Dresden (Germany)

Supporting information for this article is available on the WWW under https://doi.org/10.1002/open.202000152

years.[47–50] Numerous publications from the last years deal with the mechanisms of disproportionation of hexachlorodisilane and other chlorosilanes (see Scheme 1).[51–58] Suitable preparation methods for branched and cyclic perchlorooligosilanes have been published in connection with these works.[17] **dodecachloroneopentasilane** (neo-Si_5Cl_{12}) (**4**) and bis(tetra-*n*-butylammonium) dodecachlorocyclohexasilane bis(chloride) (**5**) were prepared on the basis of these procedures: disproportionation of Si_2Cl_6 in presence of trimethylamine gave **4** (see Scheme 1). **5** was prepared by disproportionation of Si_2Cl_6 in presence of tetra-*n*-butylammonium chloride. Those preparations have been described in the literature (for citations see above).

Further optimization of the synthesis conditions, experiments with different cations and solvents lead to several crystalline products and X-ray crystal structures of derivatives of **4** and **5**. The core features of these structures are listed in Table 1. Full details of the preparative procedures are presented elsewhere.[59,60] Crystallographic data are provided in the Supporting Information.

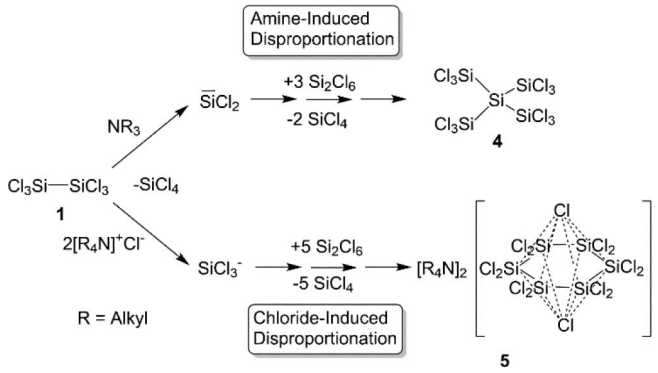

Scheme 1. Formation of **4** and **5** (R = *n*-Bu) from **1** according to mechanistic investigations from literature.[52,53]

2.2. Preparation of Hydridosilanes

Reduction of the chlorosilanes with diisobutylaluminum hydride yielded the hydridosilanes **6**, **7**, and **8** (see Scheme 2). Cyclohexasilane (**9**) was prepared from **5** by reduction with lithium aluminium hydride. Destillation under reduced pressure gave the pure hydridosilanes as colorless liquids.

2.3. How to Crystallize Pyrophoric Liquids

The hydridosilanes **6–9** are highly pyrophoric liquids at room temperature. We had to overcome several challenges in order to investigate the crystal structure of these compounds. These are: **a**) Synthesis of pure samples of the compounds. **b**) To fill these hydridosilanes into glass capillaries suitable for an X-ray diffraction experiment. **c**) To transfer the glass capillaries onto the diffractometer without breaking the glass. **d**) Getting single crystals by cooling the glass capillaries on the diffractometer. **e**) To perform the X-ray diffraction experiment, which was rather a simple task, once the single crystal was obtained.

Synthesis of the hydridosilanes (**a**) was performed in our laboratories by careful work with up-to-date Schlenk technique[62,63] (see Experimental). The transfer of the hydridosilanes into glass capillaries was performed in a glovebox under argon atmosphere (step **b**). We used sample tubes ("XRD capillaries", in German: "Markröhrchen") from Hilgenberg with 0.5 mm diameter.[64] These have low absorption through the extremely thin-walled glass, a defined inner diameter, and a wide funnel on one end to fill in the sample. The sample tubes

Table 1. Single crystal structures from X-ray diffraction determined in connection with the syntheses of halogenoligosilanes **4** and **5**.

	linearized structural formula	crystal system/ space group	cell constants
5a	$[n\text{-}Bu_4N]_2[Si_6Cl_{14}]$ 2 $C_2H_2Cl_4$	Monoclinic, $P2_1$	a = 12.0417(3) Å α = 90° b = 17.9924(4) Å β = 97.073(2)° c = 15.8081(4) Å γ = 90°
5b	$[n\text{-}Bu_4N]_2[Si_6Cl_{14}]$ 2 CH_3CN	Triclinic, P-1	a = 10.5959(7) Å α = 109.593(5)° b = 12.4915(8) Å β = 106.954(5)° c = 13.2360(8) Å γ = 96.600(5)°
5c	$[BzNEt_3]_2[Si_6Cl_{14}]$	Triclinic, P-1	a = 10.0085(6) Å α = 73.363(5)° b = 10.1418(6) Å β = 82.077(5)° c = 11.7708(7) Å γ = 86.619(5)°
5d	$[n\text{-}Pr_4N]_2[Si_6Cl_{14}]$	Triclinic, P-1	a = 11.3291(9) Å α = 93.964(7)° b = 11.6248(9) Å β = 116.155(6)° c = 12.221(1) Å γ = 116.323(6)°
5e	$[n\text{-}Bu_4N]_2[Si_6Cl_{13}Br]$	Tetragonal, $I4_1/a$	a = 17.3137(5) Å α = 90° b = 17.3137(5) Å β = 90° c = 37.859(1) Å γ = 90°
5f	$[Et_4N]_2[Si_8Cl_{18}]{\cdot}CH_2Cl_2$	Monoclinic, $P2_1/n$	a = 13.4090(7) Å α = 90° b = 12.8193(5) Å β = 92.859(4)° c = 15.2698(8) Å γ = 90°
4a	$Si(SiCl_3)_4{\cdot}SiCl_4$ [a]	Cubic, F-43c	a = 17.151(2) Å α = 90° b = 17.151(2) Å β = 90° c = 17.151(2) Å γ = 90°

[a] Redetermination of a previously published structure, see 61.

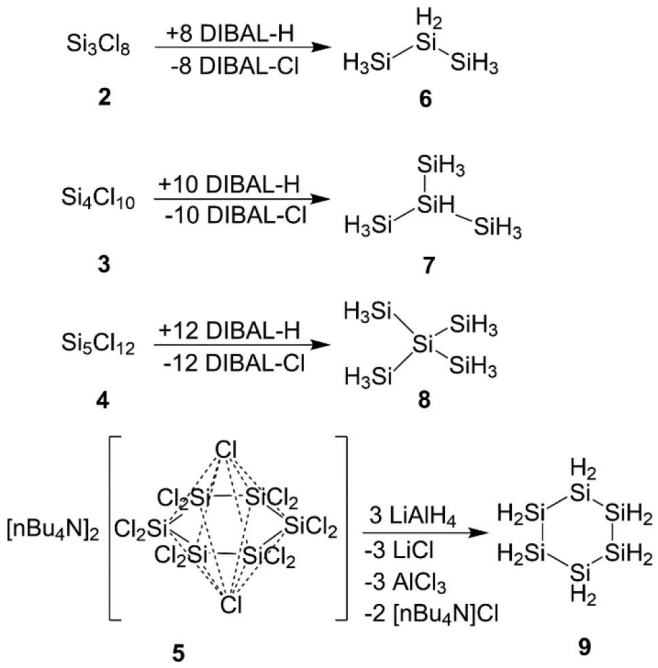

Scheme 2. Syntheses of the hydridosilanes **6**–**9**.

were supplemented with a simple but effective setup to handle the samples under inert conditions (see Figure 1). This consists of a stopcock, which is connected to a glass screw joint with GL14. The GL14 screw cap has an outlet, which is closed by a silicone septum. The sample tube is sticked through that septum, before the sample tube is filled with the liquid hydridosilane.

Filling of the sample tube is performed in the glovebox with a suitable glass needle (0.3 mm diameter) attached to a micro syringe. The stopcock with the glass screw joint is screwed onto the screw cap after filling the sample tube. This setup (closed stopcock with screw cap and filled sample tube) is removed from the glovebox. All further steps are performed at the Schlenk line. The content of the sample tube is frozen with liquid nitrogen. Vacuum is applied via the stopcock and the sample tube is sealed by melting the glass with a small gas torch. Slow heating to room temperature and storage of the sample tubes for (at least) several hours reveals, whether the tubes are sealed correctly and are safe to handle. If they are not properly sealed, the substance in the sample tube turns brown

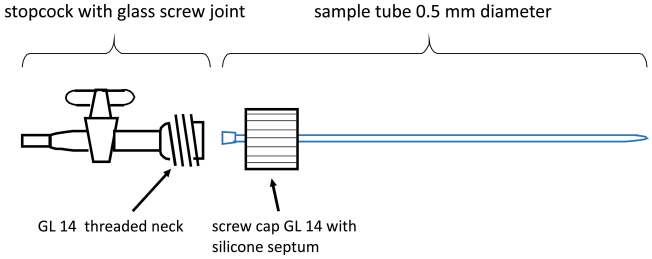

Figure 1. Setup to fill XRD capillaries with pyrophoric liquid samples.

or burns out of the glass. The sample tubes, which survived storage at room temperature, are used for the diffraction experiments. The sample tubes are glued with paraffin into a sample holder which is placed on the goniometer head (**c**). Freezing and melting of the hydridosilanes is performed with a liquid nitrogen cooling device from Oxford Cryosystems at the IPDS II X-ray diffractometer.

Growing single crystals of low-melting compounds has been practised for many years.[65–67] Different in-situ cryo crystallization techniques are described in a review by Boese and Nussbaumer.[68] A number of (at room temperature) liquid alkanes, alkynes, and other compounds have been crystallized in-situ and were analyzed as single crystals (for examples see[69–72]). Recently a special issue of Zeitschrift für Kristallographie on in-situ crystallization has been published.[73] Notwithstanding the numerous experiments and knowledge by several groups, every crystallization experiment on the diffractometer is a challenging task. Or, how Boese wrote recently: "In-situ crystallization is an art, by no way it is routine".[73]

We have cooled the substance sealed within the capillary with the nitrogen stream until crystallization occurs. The quality of the crystallized material was consistently checked with some X-ray scans and a subsequent cell search. Diffraction patterns revealed the nature of the material. The first (fast) crystallization always yields polycrystalline material. This was molten again by heating close to the melting point of the compound. We faced exactly the problems Boese has described with supersaturated solutions below the melting point.[68,73] Repeated freezing and melting procedures on the diffractometer provided single crystals of neopentasilane (**8**) and cyclohexasilane (**9**). Trisilane (**6**) and isotetrasilane (**7**) did not yield single crystals under these conditions. Therefore, a miniature zone refining was performed with the polycrystalline material of **6** and **7** by moving the capillary slowly up and down in the cooling stream. This gave single crystals at last (**d**).

The crystallization processes were monitored with a video microscope and the quality of the formed crystals were checked with X-ray scans. Details about temperature ranges for these crystallization processes are listed in Table 2. Cyclohexasilane (**9**) forms a glassy state, when it is cooled below the melting point. After trials with several solvents, a solution of cyclohexasilane with about 10% *n*-pentane yielded a suitable single crystal in the capillary.

Temperature was lowered about 10 to 30 K for the X-ray diffraction experiment (**e**) with respect to the temperature of growing single crystals. This was done in order to keep the single crystals stable in the capillary and to avoid the formation of cracks in the single crystal by cooling them further down.

2.4. Molecular Structures and Crystal Packing

Trisilane (**6**) crystallizes in the monoclinic space group I2/c with four molecules in the unit cell. An alternate setting of this space group is C2/n (for details see Experimental Section). The asymmetric unit contains a half molecule, with the silicon atom Si2 on a special position. Rotation around a C_2 axis, which goes

Table 2. Crystallization conditions for the hydridosilanes **6–9** (all values in °C).

compound	melting point with reference		temperature range for crystallization	temperature of X-ray diffraction experiment
trisilane (**6**)	−117.5	[24]	−128 to −123	−143
isotetrasilane (**7**)	−99.4	[30]	−103 to −93	−110
neopentasilane (**8**)	−57.8	[74]	−68 to −62	−93
cyclohexasilane (**9**) with 10% *n*-pentane	+16.5	[75]	−3 to +2	−30

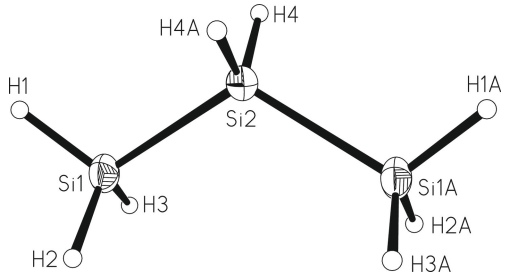

Figure 2. Molecular structure of trisilane (**6**) including numbering scheme. The thermal displacement ellipsoids of the non-hydrogen atoms are drawn at the 50% probability level.

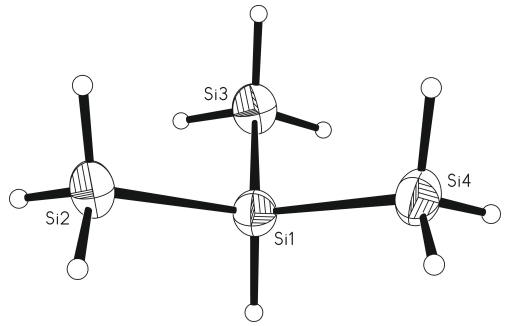

Figure 3. Molecular structure of isotetrasilane (**7**) including numbering scheme. The thermal displacement ellipsoids of the non-hydrogen atoms are drawn at the 50% probability level.

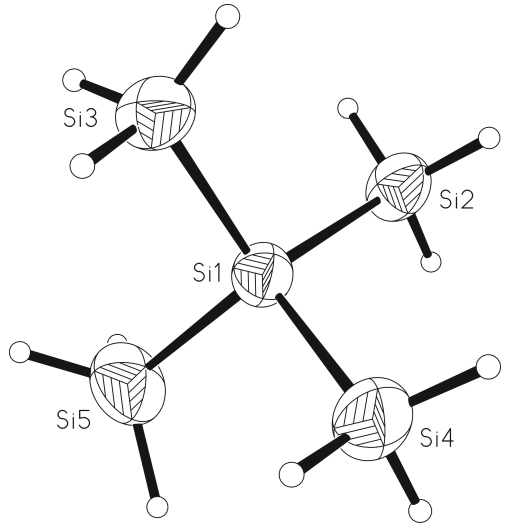

Figure 4. Molecular structure of neopentasilane (**8**) including numbering scheme. The thermal displacement ellipsoids of the non-hydrogen atoms are drawn at the 50% probability level.

through that position, generates the third silicon atom (Si1 A in Figure 2). Isotetrasilane (**7**) crystallizes in the monoclinic space group $P2_1/c$ with four molecules in the unit cell. The asymmetric unit contains one molecule (Figure 3). Neopentasilane (**8**) crystallizes in the tetragonal space group $I4_1/a$ with 16 molecules in the unit cell. The molecule structure is shown in Figure 4. Cyclohexasilane (**9**) crystallizes in the monoclinic space group C2/c with four molecules in the unit cell. The asymmetric unit contains a half molecule. Inversion at the center of the six membered ring generates the complete molecule (see Figure 5).

Only very few molecular structures of hydridosilanes are known until today. There are powder-XRD studies on layered polysilane $(Si_6H_6)_n$,[76] the crystal structure of a high-pressure phase of monosilane (SiH_4),[77] the high-pressure van-der-Waals adduct $SiH_4(H_2)_2$,[78] and the single crystal molecular structures of cyclopentasilane[38] and 2,2,3,3,4,4-hexasilylpentasilane.[19] Furthermore, molecule geometries of several hydridosilanes have been derived from gas-phase electron diffraction (see Table 3). A search within the Inorganic Crystal Structural Database (ICSD Data Release 2019.2) and the Cambridge Structural

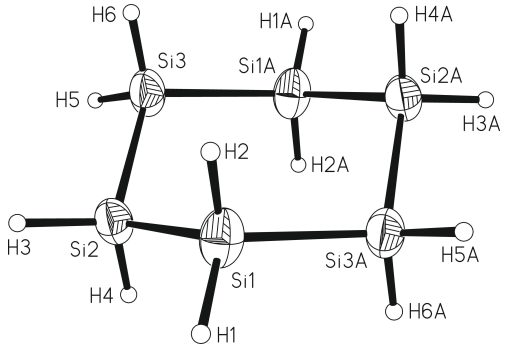

Figure 5. Molecular structure of cyclohexasilane (**9**) including numbering scheme. The thermal displacement ellipsoids of the non-hydrogen atoms are drawn at the 50% probability level.

Table 3. Structural data of hydridosilanes from gas-phase electron diffraction.

molecule	Si–Si bond length [Å]	reference
disilane, Si_2H_6	2.331(3)	[82]
trisilane, Si_3H_8	2.332(2)	[83]
n-tetrasilane, Si_4H_{10}	(terminal bond) 2.335(3) (central bond) 2.340(3)	[83]
cyclopentasilane	2.342(3)	[84]
cyclohexasilane	2.342(5)	[85]

Database (CSD version 5.41, November 2019) for compounds related to **6**, **7**, **8**, and **9** yielded to disiloxane (30501-ICSD)[79] and disilylphosphanide (CSD Refcode PIKWAH)[80] with a similar molecular structure to **6**. Trisilylamine (201428-ICSD)[81] has a similar molecular structure to **7**. No similar molecules exist for **8** and **9**.

The silicon-silicon bond lengths from the X-ray diffraction experiments (see Table 4) seem to be somewhat shorter than in the gas phase. This might be caused by the different experimental conditions, i.e. gas-phase structure versus low temperature crystal structure. Directly comparable are the bond lengths of trisilane (**6**) [gas phase: 2.332(2) Å, solid state: 2.326(1) Å] and cyclohexasilane (**9**) [gas phase: 2.342(5) Å, solid state: mean value 2.322 Å]. Three Si–Si bond lengths are given for the isotetrasilane (**7**) in Table 4. The differences between those bond lengths are not significant, that means a mean value of 2.333 Å should be used for discussion. The silicon-silicon bond lengths for neopentasilane (**8**) vary between 2.311(1) to 2.317(1) Å. A mean value of 2.314 Å should be used. This value is shorter than the Si–Si bond lengths from gas-phase electron diffraction and also the shortest bond length within this series of compounds. This is somewhat surprising, since one would assume rather longer bond lengths in **8** due to the substitution with four SiH_3 groups at one silicon atom. Quantum chemical optimizations of trisilane, isotetrasilane, and neopentasilane with M062X/6-311+G(d,p) show Si–Si bond lengths of 2.339-2.340 Å for all three molecules (for details see Supporting Information). No special short bonds for neopentasilane could be detected, also not with other method/ basis set combinations (see Supporting Information).

The single crystal structure of cyclopentasilane (**10**) has been determined before.[38] A mean value for the Si–Si bonds of 2.336 Å was listed there. The shorter bond lengths in cyclohexasilane (**9**) with a mean value of 2.322 Å might be explained with the more relaxed character of the six membered ring in comparison with a five membered ring.

The hydrogen atoms in **6–9** have been localized from residual electron-density maps and their positions were refined with Si–H bond lengths between 1.30 and 1.44 Å. Due to the weak diffraction power of hydrogen atoms with X-rays no further information can be drawn from this data.

Table 4. Silicon-silicon bond lengths (in Å) of the hydridosilanes **6–9** from single crystal X-ray structure analyses.

compound	bond	length
trisilane (**6**)	Si1-Si2	2.326(1)
isotetrasilane (**7**)	Si1-Si2	2.333(1)
	Si1-Si3	2.332(1)
	Si1-Si4	2.333(1)
neopentasilane (**8**)	Si1-Si2	2.313(1)
	Si1-Si3	2.311(1)
	Si1-Si4	2.317(1)
	Si1-Si5	2.316(1)
cyclohexasilane (**9**)	Si1-Si2	2.320(1)
	Si2-Si3	2.318(1)
	Si1-Si3A [a]	2.328(1)

[a] Symmetry transformation used to generate equivalent atoms: −x+3/2, −y+3/2, −z+1

The silicon atoms in **6–9** are in distorted tetrahedral geometry. Distortion goes – for example – in compound **6** from 107 to 116.7°. Trisilane (**6**), isotetrasilane (**7**), and neopentasilane (**8**) crystallize in the most favorable geometry (as one would expect) with all H–Si-Si–H and H–Si-Si–Si bonds in staggered conformation. Cyclohexasilane (**9**) is in chair conformation with alternating torsion angles along the chain of silicon atoms of 54.6° (Si1-Si2-Si3-Si1A), −55.5° (Si2-Si3-Si1A–Si2A), 55.6° (Si3-Si1A–Si2A–Si3A) and so on.

Intermolecular interactions are analyzed on the basis of van-der-Waals radii of silicon and hydrogen.[86,87] Three intermolecular interactions are present in the crystal structure of the trisilane (**6**), see Table 5. The interactions Si1···Si2(a) and Si1···H1 are localized within the plane of the molecule. Due to the high crystallographic symmetry every molecule in the crystal lattice features eight interactions with neighboring molecules within that plane (see Figure 6 for illustration). This hints already to a close packing of the molecules within these layers (details are discussed below). The third interaction H2···Si2(a) is close to the van-der-Waals limit and connects the layers. The molecules of isotetrasilane (**7**) are arranged in double layers of molecules, where the central hydrogen atom at Si1 is alternatively directed upwards or downwards with respect to the crystallographic a-axis. Whithin these double layer two intermolecular contacts between silicon atoms Si2 and Si3 are found (see Table 5). The closest distances between molecules of neopentasilane (**8**) are above the sum of van-der-Waals radii (see Table 5). No shorter

Table 5. Intermolecular distances of **6–9** in the solid state (in Å).

compound	interaction	length	length – r_{vdW}	symmetry operation (a)
trisilane (**6**)	Si1···Si2(a)	4.142	−0.058	x, y−1, z
	Si1···H1	3.113	−0.187	0.5−x, y−0.5, 1−z
	H2···Si2(a)	3.298	−0.002	0.5−x, 0.5−y, 1.5−z
isotetrasilane (**7**)	Si3···Si2(a)	4.158	−0.042	−x, y−0.5, 0.5−z
	Si2···Si2(a)	4.121	−0.079	−x, 1−y, 1−z
neopentasilane (**8**)	Si2···H5(a)	4.006	0.706	0.75−y, −0.75+x, −0.75+z
	H1···Si3(a)	3.516	0.216	
cyclohexasilane (**9**)	Si2···Si2(a)	4.151	−0.049	1−x, y, 0.5−z

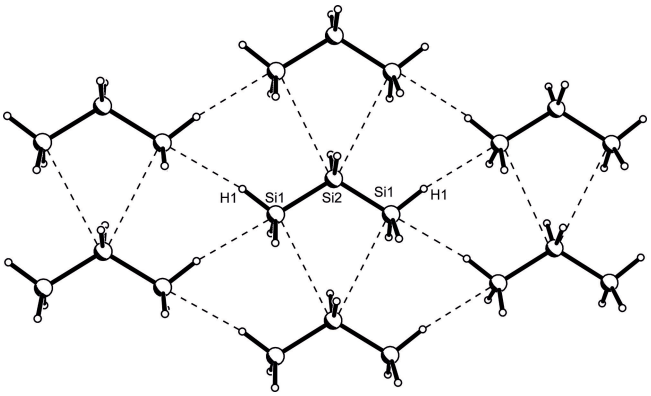

Figure 6. Intermolecular interactions in the crystal structure of trisilane (**6**).

intermolecular distances are present in this crystal structure. Therefore, one should conclude that a close packing of molecules is present in this structure without specific intermolecular interactions.[88] Cyclohexasilane (**9**) has one intermolecular contact between two neighboring atoms Si2. The contact with a length of 4.151 Å is close to the sum of van-der-Waals radii with 4.2 Å.

The crystal structures deliver also information about the packing of the molecules in the crystal lattice. The packing index (PI) is one of the most instructive parameter to describe a crystal structure.[89] This value represents a measure for the percent of filled space in a given crystal structure. The average value of PI for organic crystals is around 72%.[88] Rigid spheres in closest contact reach values of 74%.[90] The packing indices for compounds **6–10** are shown in Table 6 together with the indices of some structural related alkanes.

First glimpse on these data reveals that the hydridosilanes have higher packing indices than the corresponding alkanes. Reasons for that might be found from a comparison of packing patterns between corresponding alkanes and hydridosilanes. Propane features a loosely packed arrangement of irregular pentagons with a packing index of 63.3% (see Figure 7, left).[93] In contrast to that, trisilane has a completely different packing pattern. The shape of the molecules therein is best described as shevron. These are able to pack in one plane, one after the other, all orientated in the same direction, thereby reaching a packing index of 70.9% (see Figure 7, right).

Why are the shape of propane and trisilane so different? To understand this question one might want to look at the van-der-Waals radii of the three elements hydrogen, carbon and silicon (see Table 7 and Figure 8).[86,87] The ratio of the volume V_E/V_H is 1:2.8 for hydrogen and carbon and 1:5.4 for hydrogen and silicon. That means the overall shape of alkanes is also formed by the position of the hydrogen atoms at surface of the carbon skeleton. In case of the hydridosilanes the overall shape of the molecules is dominated by the arrangement of silicon atoms. The hydrogen atoms play a minor role, since they are merely "tiny dots" at the surface of the hydridosilane. The packing pattern of the trisilane confirms this assumption.

The packing patterns of isotetrasilane (**7**) and neopentasilane (**8**) are shown in Figure 9. Isotetrasilane (**7**) forms a double layer of molecules with the central hydrogen atoms pointing alternatively up and down. The packing index of these "tripodal" molecules is 67.3%. An even lower packing index of 65.4% is observed in the tetrahedral molecules of neopentasilane (Figure 8, right). No layer structure can be found here, instead a three-dimensional arrangement of molecules is observed.

Figure 10 shows the comparison of packing patterns of cyclohexasilane (**9**) and cyclohexane. The shape of both molecules can be described with regular hexagons. These hexagons are arranged in a different way in both structures. The resulting packing indices are 68.5% in cyclohexane and 74.3% in cyclohexasilane (**9**), which indicates a more effective packing in the latter one. This might be ascribed to the more pronounced hexagonal shape of the cyclohexasilane molecules

Table 6. Packing indices (PI in %) of **6**–**10** and related alkanes from literature.

silanes	PI	alkanes	PI
trisilane (**6**)	70.9	propane[69]	63.3
isotetrasilane (**7**)	67.3		
neopentasilane (**8**)	65.4		
cyclohexasilane (**9**)	74.3	cyclohexane[91]	68.5
cyclopentasilane (**10**)[38]	70.1	cyclopentane[92]	68.6

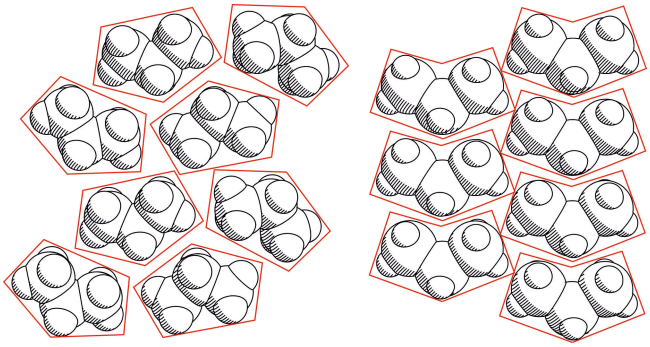

Figure 7. Layer structure in propane (left) and trisilane (**6**, right).

Table 7. Van-der-Waals radii, volume, ratio of volume of hydrogen, carbon and silicon atoms.

atom	H	C	Si
van-der-Waals radius (Å)	1.2	1.7	2.1
volume (Å^3)	7.24	20.58	38.79
ratio of volume V_E/V_H	1	2.8	5.4

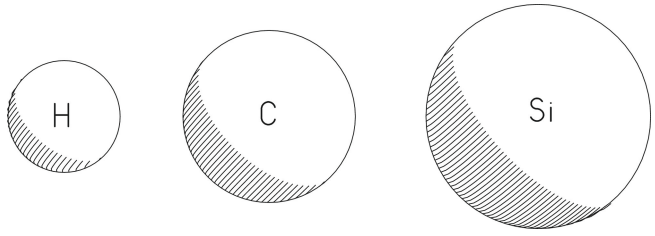

Figure 8. Visual representation of the volumes of hydrogen, carbon, and silicon atoms.

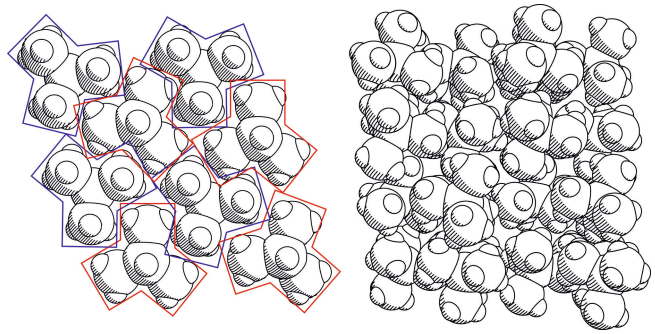

Figure 9. Packing pattern of isotetrasilane (**7**, left) and neopentasilane (**8**, right).

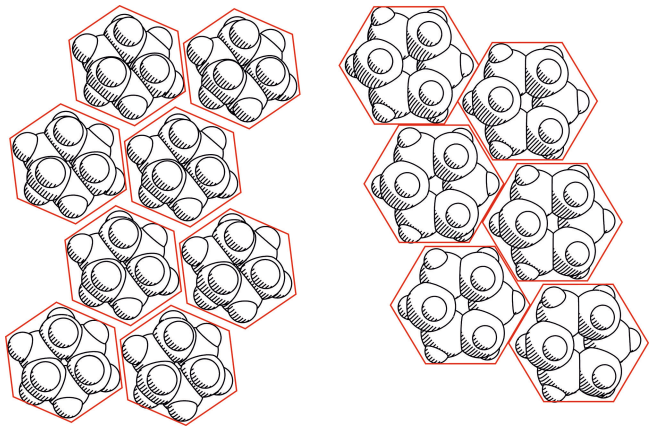

Figure 10. Packing pattern of cyclohexane (left) and cyclohexasilane (**9**, right).

featuring small "dots" of hydrogen on their surface (see discussion above).

The differences in the packing indices of cyclopentane and cyclopentasilane (**10**) are not so big with values of 68.6 and 70.1 % respectively, but also present. The crystal structure of cyclopentasilane has been published before,[38] therefore we abstain from a detailed discussion of this structure.

2.5. Radiation Experiments in Combination with Spectroscopy

Irradiation of hydridosilanes is the first step during the liquid phase deposition of silicon (Scheme 3). Under the influence of UV-light, high temperature or ultrasonic treatment molecular hydridosilanes form soluble oligomers. These oligosilanes are also known as "liquid silicon" or "silicon ink" and can be deposited as thin films for example by spin coating. The oligosilanes can be converted into amorphous and polycrystalline silicon by further thermal or laser treatment. The resulting silicon films are the starting point for the preparation of thin film solar cells, thin film transistors or other electronic devices. We recently reported a detailed study about the polymerization of CPS by irradiation.[16] Here we investigated the irradiation of **9**.

In a standard Schlenk flask a 25 % solution of **9** in tetrahydronaphthalene (THN) is stirred and irradiated with UV-light (365 nm) through the glass. After 0, 5, 10, 15, 20 and 45 min respectively, a sample was taken for ^{29}Si-NMR investigation (Figure 11). During the irradiation the clear colourless solution turns slightly yellow. Between 15 and 20 min a white precipitate is formed.

The longer the irradiation of the solution takes place, the lower is the signal of **9** (Figure 11 b)) in the ^{29}Si-NMR spectrum. In contrast, the intensity of signals indicating SiH_3-groups (Figure 11a)) and SiH_2-groups in chain-like hydrosilanes (Figure 11c)) increases. They are already detectable after five minutes of irradiation. Signals indicating SiH branching units (Figure 11d)) or quarternary Si atoms (Figure 11e)) are not seen after 160 scans. So, the spectrum of the sample, which was irradiated for 15 min was measured again with 1000 scans (Figure SI2). Under these conditions a weak signal indicating a SiH crosslinking unit is detected. The existence of such SiH structural moieties was proven by comparing DEPT-135 (Figure SI3) and DEPT-90 ^{29}Si-NMR spectra (Figure SI4) of the sample. Due to the NMR experimental settings, in the DEPT-90 spectrum the intensity of the SiH groups is maintained whereas the other signals are suppressed. Therefore, the comparison of the DEPT ^{29}Si-NMR spectra confirm the formation of SiH crosslinking moieties. Signals of quaternary Si atoms are still not seen in the spectra. There could be different reasons. Either the concentration is too small for ^{29}Si-NMR (natural abundance of ^{29}Si: 4.67 %)[94] or the highly branched hydridosilanes precipitate and are no longer detectable in the solution. However, the ^{29}Si-NMR spectra clearly show the formation of branched and chain-like oligosilanes under consumption of cyclohexasilane (**9**) during the irradiation.

For further insight into the mechanism of the polymerisation of **9** by irradiation with UV-light we used in-situ ESR spectroscopy. Therefore, pure **9** in a sealed quartz capillary was irradiated with 365 nm directly in the resonator of an ESR spectrometer. With the start of the irradiation a signal indicating a paramagnetic species was observed immediately (Figure 12). This can be attributed to various silyl radicals or triplet silylenes. The g-value was determined to $g = 2.0053$. That indicates silyl radicals in branched hydridosilanes.[95–97] The signal is relatively weak and shows no hyperfine coupling. The missing of hyperfine coupling further indicates the absence of hydrogen, which is connected to the Si atom with the unpaired electron.[98] Due to the g-value and the absent hyperfine coupling in the ESR spectra from **9** during irradiation, the detected silyl radicals were preferably located on tertiary Si atoms. With longer irradiation time the concentration of paramagnetic species

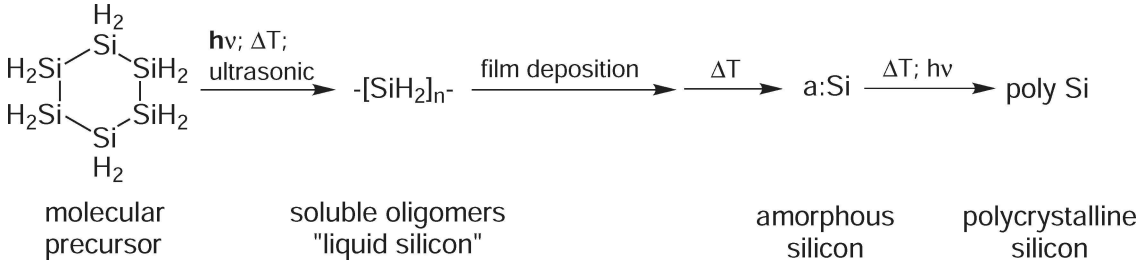

Scheme 3. Simplified illustration of solution-based formation of Si films, with cyclohexasilane (**9**) as starting material.

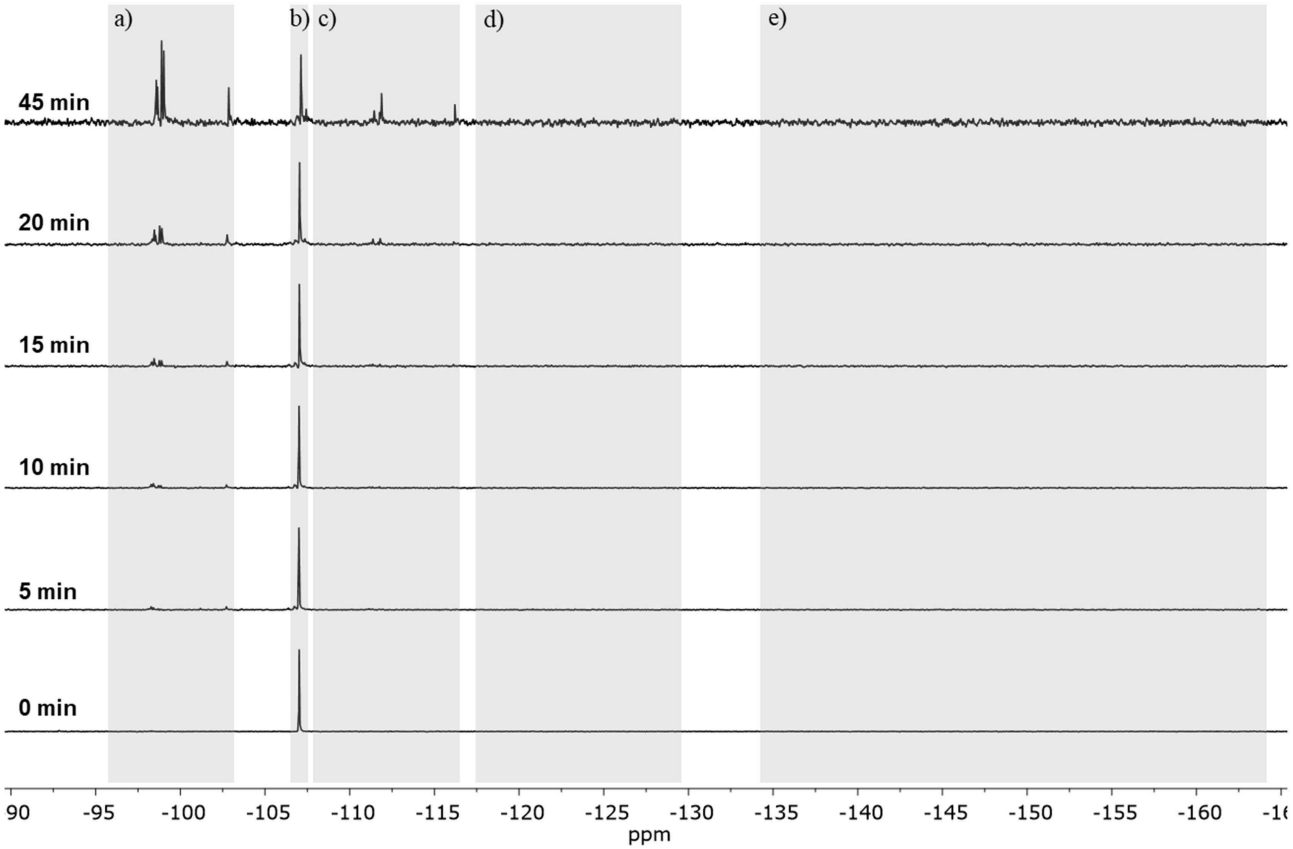

Figure 11. ^{29}Si-IGATED-NMR spectra (160 scans) of cyclohexasilane (**9**) in THN and irradiated solutions of **9** after different periods of time. The grey areas indicate the chemical shift region for a) SiH_3 units, b) **9** or other SiH_2 units in cyclic hydridosilanes, c) SiH_2 units in chain-like hydridosilanes, d) SiH crosslinking units and e) quaternary Si units in hydridosilanes.

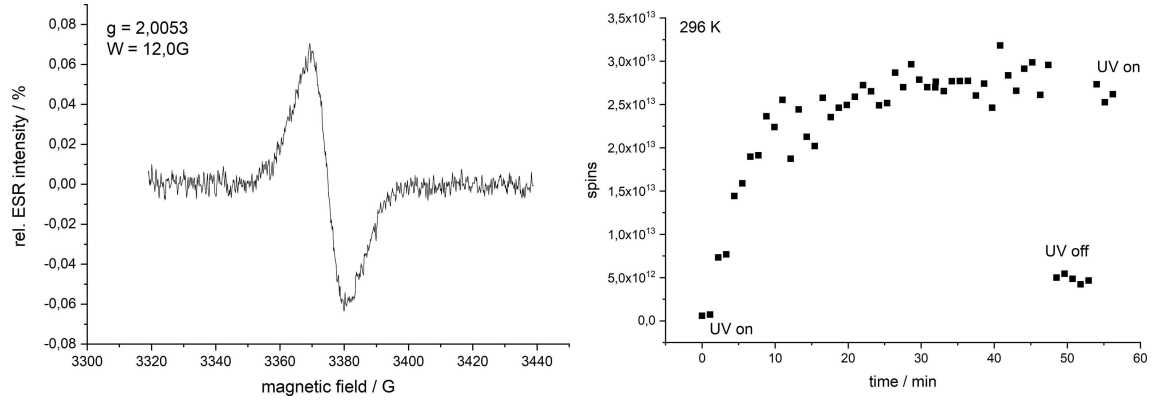

Figure 12. ESR spectrum of pure **9** during irradiation with 365 nm (left) and the detected paramagnetic species over the time of irradiation (right).

increases and approaches a saturation concentration (Figure 12), which stays constant as long as the irradiation was continued. As soon as the irradiation was stopped the paramagnetic species cannot be observed any longer. By continuing the irradiation, the concentration of the paramagnetic species increased up to the saturation concentration immediately. Cyclopentasilane (**10**) shows a very similar behaviour compared to **9** during irradiation.[16]

The compounds **6**, **7**, and **8** were filled in quartz capillaries and treated with UV-light at 365 nm. The liquids remained unchanged. That means these three compounds cannot be oligo- and polymerized under these conditions.

2.6. Thermal Stability of 9

The thermal decomposition of **9** starts at 110 °C. That is very similar to the decomposition temperature of **10**.[38] After a mass loss of about 80% the decomposition is completed at 170 °C. This great mass loss in a relatively narrow temperature range is surprisingly similar to branched hydrosilanes like 2,2,3,3-tetrasilyltetrasilane or 2,2,4,4-tetrasilylpentasilane.[14] Unfortunately **6**, **7**, and **8** could not be transferred in the TG/DTA without burning off.

3. Conclusions

Although hydridosilanes are already known for more than one hundred years only very few crystal structures of such compounds are published. We were able to determine the molecule structures of some basic hydridosilanes. This data gives information about bond parameters in the solid state and shows packing patterns which differ substantially from the structurally related alkanes. The packing indices PI for trisilane (**6**), cyclohexasilane (**9**) and cyclopentasilane (**10**) are significantly higher than the PI values for the corresponding alkanes. This is accompanied by some H…Si and Si…Si interactions with distances below the sum of the van-der-Waals radii.

Usage of these hydridosilanes as "liquid silicon" or a "silicon ink" requires the transformation of these precursors under the influence of UV-light, high temperature or ultrasonic. The first steps of transforming cyclohexasilane (**9**) into a mixture of soluble oligomers were investigated in this work: Irradiation of **9** with UV-light delivers radicals. Tertiary silyl radicals were detected by an irradiation experiment in combination with ESR spectroscopy. Time-dependent ^{29}Si-NMR spectroscopy clearly shows the formation of branched and chain-like oligosilanes under consumption of cyclohexasilane (**9**) during the irradiation. DEPT ^{29}Si-NMR spectra prove the formation of SiH crosslinking moieties by irradiation.

Cyclohexasilane (**9**) is a little bit easier to handle than the other hydridosilanes described in this paper. Our preparative approach delivers several grams of this compound in one batch. Therefore, we think that **9** is a suitable precursor to generate "liquid silicon ink".

Experimental Section

All reactions were performed in a dry argon or nitrogen atmosphere by using standard Schlenk or glovebox techniques. The chemicals were purchased from commercial sources. Hexachlorodisilane, Si_2Cl_6 (**1**), octachlorotrisilane, Si_3Cl_8 (**2**), perhalogenated isotetrasilane, $ClSi(SiCl_3)_3$ (**3**) were bought from Nagarjuna Spawnt GmbH, 06766 Bitterfeld-Wolfen, Germany.

Dichloromethane, diethylether, and *n*-hexane were dried prior to use in a solvent purification system by MBRAUN. Benzene and tetrahydronaphthalene (THN) were freshly distilled from sodium. All solvents were stored over 4 Å molecular sieves until usage. Analytic measurements include nuclear magnetic resonance spectroscopy, ESR spectroscopy, elemental analysis, and structure determination by X-ray crystallography. ^{29}Si NMR spectra of liquid samples were recorded with a BRUKER Avance III 500 MHz and a BRUKER Nanobay 400 MHz spectrometer with resonance frequencies of 99.36 or 75.62 MHz, respectively. Tetramethylsilane [$\delta(^{29}Si) = 0$ ppm] was used as internal standard.

Inverse gated decoupling experiments with a recycle delay of 30 s were recorded for the NMR investigation of the irradiated samples. In the DEPT (Distortionless Enhancement by Polarization Transfer) experiments, the evolution period was set to 2.5 ms [$J(^{29}Si,^{1}H) = 200$ Hz] and the recycle delay to 5 s. The value of the 90° pulse was 13.8 µs for ^{29}Si and 8.85 µs for ^{1}H. The length of the 90° (DEPT-90) and the 135° (DEPT-135) read pulse was calculated from the 90° pulse of ^{1}H.

The elemental analysis was performed with an Elementar varioMICRO instrument with tin capsules as sample container.

The in-situ ESR measurements were performed in a BRUKER EMX plus X-Band CW ESR spectrometer with a high sensitivity resonator ER4119HS and an internal temperature control unit (ER 4131VT). A NMR teslameter (ER036TM) was used for g-value-determination. The TG/DTA measurements were performed on a Setaram Sensys TG-DSC in a temperature range from 20 to 500 °C with a heating rate of 5 K/min. Argon was used as carrier gas (flow rate: 20 ml/min) and the samples were transferred in Al_2O_3 crucibles.

Synthesis of dodecachloroneopentasilane (4): In a representative experiment, a Schlenk flask was charged with 13 ml Si_2Cl_6 (20 g; 74 mmol). Under iso-propanol/dry ice cooling 0.1 g of a nitrogen-containing base ($EtMe_2N$, Py, Et_3N) were added. The cooling was removed and the mixture was stored at room temperature for several days. Colorless octahedral crystals with edge lengths of up to 1 cm were formed inside the solution. $SiCl_4$, a byproduct of the reaction, was removed under reduced pressure. After sublimation of the crystalline solid under reduced pressure at 200 °C oil bath temperature Si_5Cl_{12} was obtained as a colorless solid in yields of up to 73% (7.64 g).

An analogous synthesis with Si_3Cl_8 as starting material also gives Si_5Cl_{12} in equally good yields.

For X-ray structure determination crystals of $Si_5Cl_{12}{\cdot}SiCl_4$ are collected directly from the reaction mixture of the disproportionation. Recrystallization from benzene leads to single crystals suitable for X-ray structure determination, as well.[99]

^{29}Si NMR (C_6D_6) $\delta = 3.9$ ppm $(\mathbf{Cl_3Si})_4Si$; -80.2 ppm $(Cl_3Si)_4\mathbf{Si}$

Synthesis of $[n\text{-}Bu_4N]_2[Si_6Cl_{14}]$ (5): In a representative experiment, a Schlenk ampoule was charged with $[n\text{-}Bu_4N]Cl$ (12.22 g, 44 mmol). The solid was dried in a dynamic vacuum for several hours. Afterwards, the dry salt was fully dissolved in CH_2Cl_2 (50 ml) to produce a clear colorless liquid. After freezing the solution in liquid nitrogen neat Si_2Cl_6 (22.70 ml, 35.46 g, 131.9 mmol) was added without stirring. Then the ampoule was vacuum-sealed and slowly heated up to room temperature, causing the colorless liquid to adopt a pale yellow color. The sealed ampoule was stored in an explosion-proof metal pipe and heated up to 85 °C in a drying oven for the next 24 h. Afterwards the ampoule was allowed to cool down in the oven. After opening the ampoule, an equal volume of benzene was added to the mixture forming a white precipitate immediately. The suspension was stirred for 24 h and filtered afterwards. The white solid was identified as pure $[n\text{-}Bu_4N]_2[Si_6Cl_{14}]$ in a yield of up to 35% (8.78 g).

^{29}Si NMR (C_6D_6) $\delta = -22.3$ ppm

Anal calc. for $C_{32}H_{72}Cl_{14}N_2Si_6$ (1149.79): calc. N 2.44%, C 33.43%, H 6.31%; found N 2.40%, C 33.53%, H 6.182%.

Warning: The experiments described below include work with pyrophoric silanes! Do not use $LiAlH_4$ for the preparation of **6**, **7**, and **8**! It leads to massive decomposition reactions and SiH_4 formation. During the reduction with DIBAL–H only very small amounts of SiH_4 are formed. Synthesis of cyclohexasilane (**9**) is possible with $LiAlH_4$. Small amounts of SiH_4 are formed during that reaction. Pressure due to formed gaseous side products of the reduction reactions should be released via a silicone oil filled bubble counter. Pyrophoric gases burn off at the outlet of the bubble counter. It is inalienable that this happens in a controlled way inside a fume hood and by diluting the gases with argon.

These experiments are not for the faint-hearted, since small flames always come out of the Schlenk vessels, when opened in presence of an inert gas stream!

Synthesis of trisilane (6), isotetrasilane (7) and neopentasilane (8): In a general synthesis a Schlenk flask was loaded with 25 mmol of the chlorinated silane. Under ice cooling a slight excess of the stoichiometric amount DIBAL–H was added dropwise. After full addition of DIBAL–H, the mixture was stirred for 3 h at ice bath temperatures. Afterwards the solution was stirred for another 6 h at room temperature. Distillations under reduced pressure at room temperature lead to the products as colorless, clear, pyrophoric liquids in yields up to 86%.

trisilane (**6**): 1.98 g, ^{29}Si NMR (C_6D_6) δ = −100.3 ppm ($\mathbf{H_3Si})_2SiH_2$; −117.5 ppm $(H_3Si)_2\mathbf{Si}H_2$

isotetrasilane (**7**): 2.63 g, ^{29}Si NMR (C_6D_6) δ = −95.7 ppm ($\mathbf{H_3Si})_3SiH$; −137.4 ppm $(H_3Si)_3\mathbf{Si}H$

neopentasilane (**8**): 3.28 g ^{29}Si NMR (C_6D_6) δ = −90.4 ppm ($\mathbf{H_3Si})_4Si$; −165.7 ppm $(H_3Si)_4\mathbf{Si}$

Synthesis of cyclohexasilane (9): In a Schlenk flask 20 g [*n*-$Bu_4N]_2[Si_6Cl_{14}]$ (17.4 mmol) were suspended in 140 ml dry dichloromethane and stirred under ice cooling. To this mixture 32 ml of a 4 M $LiAlH_4$ solution in diethylether (130.6 mmol) were added dropwise. Afterwards the mixture was stirred at ice bath temperatures for one hour. Then about 200 ml dry *n*-hexane were added while stirring. Dichloromethane and diethylether were removed under reduced pressure (20 kPa) and ice bath temperatures. The white solids $AlCl_3$, LiCl and unreacted $LiAlH_4$ were removed via filtration. Concentration of the filtrate under ice bath temperatures at 10–15 kPa gives an oily residue. Distillation under reduced pressure at ice bath temperatures obtained the product Si_6H_{12} as a colorless, clear, pyrophoric liquid in yields up to 70% (2.2 g).

^{29}Si NMR (C_6D_6) δ = -107 ppm ($H_{12}Si_6$)

X-ray structure determination: Details of the in-situ cryo crystallization are provided in the main text. Data collections were performed on a STOE IPDS-II image plate diffractometer equipped with a low-temperature device with Mo–Kα radiation (λ = 0.71073 Å) using ω and ϕ scans. The size of the crystals formed inside the XRD capillaries from Hilgenberg was about 0.5×0.48×0.48 mm. Software for data collection: X-AREA, cell refinement: X-AREA and data reduction: X-RED.[100] Preliminary structure models were derived by direct methods[101] and the structures were refined by full-matrix least-squares calculations based on F^2 for all reflections using SHELXL.[102] Hydrogen atoms have been localized from electron density maps. The positions of H-atoms have been refined without constraints for **6**, **7**, and **9**. The refinement of H-atom positions in neopentasilane (**8**) was performed with restraints on silicon atom Si5. Absorption correction was performed by integration.[100] The data of isotetrasilane (**7**) have been refined as two component twin with the twin matrix {−1 0 0 0 −1 0 0 0 1} and a batch scale factor of 0.51.

Further crystallographic data are listed in Table 8.

Table 8. Crystallographic and structure refinement data for **6**–**9**.

	Trisilane (**6**)	Isotetrasilane (**7**)
Empirical formula	Si_3H_8	Si_4H_{10}
Formula weight	92.33	122.44
Temperature/K	130	163
Crystal system, space group	Monoclinic I2/c	Monoclinic $P2_1/c$
a/Å	9.371(2)	4.9326(4)
b/Å	4.8593(6)	11.740(1)
c/Å	13.321(3)	13.967(1)
α/°	90	90
β/°	95.17(2)	90.046(6)
γ/°	90	90
Volume/Å^3	604.1(2)	808.8(1)
Z	4	4
ρ_{calc} (g/cm^3)	1.015	1.006
Absorption coefficient/ mm^{-1}	0.619	0.616
F(000)	200	264
Reflections collected/ unique	2999/ 629 [R(int) = 0.0266]	9793/ 1838 [R(int) = 0.0635]
Data/restraints/parameters	629/ 0/ 32	1838/ 0/ 78
Goodness-of-fit on F^2	1.332	1.109
Final R indices [I > 2sigma(I)]	R1 = 0.0276, wR2 = 0.0715	R1 = 0.0210, wR2 = 0.0561
R indices (all data)	R1 = 0.0297, wR2 = 0.0736	R1 = 0.0220, wR2 = 0.0588
Extinction coefficient	0.019(4)	n/a
Largest diff. peak and hole/e·Å^{-3}	0.269 and −0.253	0.199 and −0.184
	Neopentasilane (**8**)	Cyclohexasilane (**9**)
Empirical formula	Si_5H_{12}	Si_6H_{12}
Formula weight	152.55	180.64
Temperature/K	180	243
Crystal system, space group	Tetragonal $I4_1/a$	Monoclinic C2/c
a/Å	21.6368(7)	14.3888(12)
b/Å	21.6368(7)	8.2984(8)
c/Å	8.6250(3)	9.3307(8)
α/°	90	90
β/°	90	105.074(7)
γ/°	90	90
Volume/Å^3	4037.8(3)	1075.79(17)
Z	16	4
ρ_{calc} (g/cm^3)	1.004	1.115
Absorption coefficient/ mm^{-1}	0.617	0.694
F(000)	1312	384
Reflections collected/ unique	18919/2318 [R(int) = 0.0303]	7743/ 1221 [R(int) = 0.0210]
Data/restraints/parameters	2318/13/61	1221/ 0/ 53
Goodness-of-fit on F^2	1.158	1.142
Final R indices [I > 2sigma(I)]	R1 = 0.0543, wR2 = 0.1330	R1 = 0.0323, wR2 = 0.0747
R indices (all data)	R1 = 0.0656, wR2 = 0.1468	R1 = 0.0351, wR2 = 0.0778
Extinction coefficient	n/a	0.016(3)
Largest diff. peak and hole/e·Å^{-3}	0.587 and −0.560	0.270 and −0.416

The space group I2/c for compound **6** sounds rather unusual. An alternate setting for this crystal structure is C2/n with cell constants a = 15.581(3) Å, b = 4.8593(6) Å, c = 9.371(2) Å, and β = 121.63(1)°. Therein the angle β is larger than in I2/c. Data sets with both space group settings have been deposited.

Deposition Number 1991497–1991500 (for **6–9**), and 1991540–1991546 (for **4a** and **5a-f**) contain the supplementary crystallographic data for this paper. These data are provided free of charge by the joint Cambridge Crystallographic Data Centre and Fachinformationszentrum Karlsruhe Access Structures service www.ccdc.cam.ac.uk/structures.

UV Irradiation Experiments

A 25% solution of **9** in tetrahydronaphtalene, stirred in a standard Schlenk flask, was treated with 365 nm UV-light. After 0, 5, 10, 15, 20 and 45 min a sample was extracted for NMR investigations. C_6D_6 was used as deuterated solvent. For in-situ ESR investigations the pure cyclohexasilane in a sealed quartz capillary was directly irradiated in the ESR resonator during measurement. The experiments were performed at room temperature for up to 1 h. For this investigations a DYMAX BlueWave™ 50 was used as UV-light source.

Acknowledgements

The authors thank Beate Kutzner (NMR), Ute Groß (elemental analysis), Dr. Jürgen Seidel, and Bianca Störr (TG). U.B. thanks Dr. Jens Meyer from STOE for sharing information about the IPDSII. U.B. thanks the computing centre of the TU Bergakademie Freiberg for computing time at the High Performance Compute Cluster.

Conflict of Interest

The authors declare no conflict of interest.

Keywords: Hydridosilanes · chlorooligosilanes · crystal structure · in-situ crystallization

[1] Silanes of the general composition Si_xH_y are also denoted as "binary silicon-hydrogen compounds", "silicon hydrides", "hydrosilanes", or "oligosilanes". Unfortunately, the term "silanes" is also often used for other compounds with four substitutents on silicon.
[2] W. Simmler: "Silicon Compounds, Inorganic" in Ullmann's Encyclopedia of Industrial Chemistry. Weinheim: Wiley-VCH. doi:10.1002/14356007.a24_001.
[3] H. J. Klockner, P. Panster, P. Kleinschmit: Process for the dismutation of chlorosilanes, EP411471 (A1), 1991.
[4] T. Shimoda, Y. Matsuki, M. Furusawa, T. Aoki, I. Yudasaka, H. Tanaka, H. Iwasawa, D. Wang, M. Miyasaka, Y. Takeuchi, *Nature* **2006**, *440*, 783–786.
[5] J. J. Schneider, J. Engstler, *Nachr. Chem.* **2007**, *55*, 634–638.
[6] S. Han, X. Dai, P. Loy, J. Lovaasen, J. Huether, J. M. Hoey, A. Wagner, J. Sandstrom, D. Bunzow, O. F. Swenson, I. S. Akhatov, D. L. Schulz, *J. Non-Cryst. Solids* **2008**, *354*, 2623–2626.
[7] G. R. S. Iyer, E. K. Hobbie, S. Guruvenket, J. M. Hoey, K. J. Anderson, J. Lovaasen, C. Gette, D. L. Schulz, O. F. Swenson, A. Elangovan, P. Boudjouk, *ACS Appl. Mater. Interfaces* **2012**, *4*, 2680–2685.
[8] T. Bronger, P. H. Wöbkenberg, J. Wördenweber, S. Muthmann, U. W. Paetzold, V. Smirnov, S. Traut, Ü. Dagkaldiran, S. Wieber, M. Cölle, A. Prodi-Schwab, O. Wunnicke, M. Patz, M. Trocha, U. Rau, R. Carius, *Adv. Energy Mater.* **2014**, *4*, 1301871.
[9] T. Shimoda, T. Masuda, *Jpn. J. Appl. Phys.* **2014**, *53*, No. 02BA01.
[10] S. Guruvenket, J. M. Hoey, K. J. Anderson, M. T. Frohlich, R. A. Sailer, P. Boudjouk, *Thin Solid Films* **2015**, *589*, 465–471.
[11] A. P. Cádiz Bedini, S. Muthmann, J. Flohre, B. Thiele, S. Willbold, R. Carius, *Macromol. Chem. Phys.* **2016**, *217*, 1655–1660.
[12] H. Frey, R. Lauth, H. R. Khan, N. Eisenreich, A. Koleczko, *Phys. Sci. Int. J.* **2017**, *14*, 33788.
[13] Y. Han, K. Anderson, E. K. Hobbie, P. Boudjouk, D. S. Kilin, *J. Phys. Chem. Lett.* **2018**, *9*, 4349–4354.
[14] V. Christopoulos, M. Rotzinger, M. Gerwig, J. Seidel, E. Kroke, M. Holthausen, O. Wunnicke, A. Torvisco, R. Fischer, M. Haas, H. Stueger, *Inorg. Chem.* **2019**, *58*, 8820–8828.
[15] T. Shimoda: Nanoliquid Processes for Electronic Devices, Springer Nature Singapore Pte Ltd. **2019**. https://doi.org/10.1007/978-981-13-2953–1.
[16] M. Gerwig, A. S. Ali, D. Neubert, U. Böhme, M. Rosenkranz, A. Popov, I. Ponomarev, M. Jank, E. Brendler, L. Frey, P. Kroll, E. Kroke: From cyclopentasilane to thin film transistors, *Adv. Electron. Mater.*, submitted.
[17] H. Stueger, T. Mitterfellner, R. Fischer, C. Walkner, M. Patz, S. Wieber, *Chem. Eur. J.* **2012**, *18*, 7662–7664.
[18] T. Sontheimer, D. Amkreutz, K. Schulz, P. H. Wöbkenberg, C. Guenther, V. Bakumov, J. Erz, C. Mader, S. Traut, F. Ruske, M. Weizman, A. Schnegg, M. Patz, M. Trocha, O. Wunnicke, B. Rech, *Adv. Mater. Interfaces* **2014**, *1*, 1300046.
[19] M. Haas, V. Christopoulos, J. Radebner, M. Holthausen, T. Lainer, L. Schuh, H. Fitzek, G. Kothleitner, A. Torvisco, R. Fischer, O. Wunnicke, H. Stueger, *Angew. Chem. Int. Ed.* **2017**, *56*, 14071–14074; *Angew. Chem.* **2017**, *129*, 14259–14262.
[20] J. Sun, B. Zhang, H. E. Katz, *Adv. Funct. Mater.* **2011**, *21*, 29–45.
[21] H. Stueger, T. Mitterfellner, R. Fischer, C. Walkner, M. Patz, S. Wieber, *Inorg. Chem.* **2012**, *51*, 6173–6179.
[22] R. Kawajiri, H. Takagishi, T. Masuda, T. Kaneda, K. Yamazaki, Y. Matsuki, T. Mitani, T. Shimoda, *J. Mater. Chem. C.* **2016**, *4*, 3385–3395.
[23] A. Stock, C. Somieski, *Ber. Dtsch. Chem. Ges.* **1916**, *49*, 111–157. doi:10.1002/cber.19160490114.
[24] A. Stock, P. Stiebeler, F. Zeidler, *Ber. Dtsch. Chem. Ges.* **1923**, *56B*, 1695–1705. doi:10.1002/cber.19230560735.
[25] A. Stock, *Zeitschrift für Elektrochemie und angewandte physikalische Chemie*, **1926**, *32*, 341–349. doi:10.1002/bbpc.19260320710.
[26] E. Wiberg, *Pure Appl. Chem.* **1977**, *49*, 691–700.
[27] A. Stock, Hydrides of Boron and Silicon, Cornell University Press, 1933, pp.173.
[28] M. Baudler, *Eur. J. Inorg. Chem.* **1998**, 2089–2105.
[29] F. Fehér, D. Schinkitz, J. Schaaf, *Z. Anorg. Allg. Chem.* **1971**, *383*, 303–313.
[30] F. Fehér, P. Hädicke, H. Frings, *Inorg. Nucl. Chem. Lett.* **1973**, *9*, 931–936.
[31] F. Fehér, D. Skrodzki, *Inorg. Nucl. Chem. Lett.* **1974**, *10*, 577–579.
[32] F. Fehér, I. Fischer, *Z. Allg. Anorg. Chem.* **1976**, 421, 9–14.
[33] F. Fehér, F. Ocklenburg, D. Skrodzki, *Z. Naturforsch. B* **1980**, *35*, 869–872.
[34] J. Hahn, *Z. Naturforsch.* **1980**, 282–296.
[35] B. Hidding, Diploma Thesis. Universität der Bundeswehr München, Heinrich-Heine-Universität Düsseldorf, **2004**.
[36] B. Hidding, C. Bruno, P. Lorenz, D. Simone, F. Klaus, N. Eisenreich, C. Hundsdörfer, A. Kornath, A. Kaufmann, S. M. Hadjizadeh, T. Soltner, T. Klapötke, M. Fikri, C. Schulz, S. Dürrstein, M. Bozkurt, X. Zhu, M. Möller, F. Vergine, C. Scharlemann, M. Pfitzner, M. Lang, G. Langel, H. Ellerbrock, J. Delis, R. Wagner: Recent activities in silicon hydride research in Europe, 2011, 17th AIAA International Space Planes and Hypersonic Systems and Technologies Conference **2011**. Reston, VA., 2287 https://doi.org/10.2514/6.2011–2287.
[37] H. Buff, F. Wöhler, *Liebigs Ann. Chem.* **1857**, *104*, 94–109. DOI: 10.1002/jlac.18571040108.
[38] D. Schmidt, U. Böhme, J. Seidel, E. Kroke, *Inorg. Chem. Commun.* **2013**, *35*, 92–95.
[39] R. Richter, G. Roewer, U. Böhme, K. Busch, F. Babonneau, H. P. Martin, E. Müller, *Appl. Organomet. Chem.* **1997**, *11*, 71–106.
[40] W. Palitzsch, U. Böhme, G. Roewer, *J. Organomet. Chem.* **1997**, *540*, 83–88.

[41] W. Palitzsch, U. Böhme, G. Roewer, *J. Organomet. Chem.* **1998**, *552*, 213–219.
[42] U. Böhme, B. Günther, B. Rittmeister, *Eur. J. Inorg. Chem.* **2003**, 751–758.
[43] B. Meinel, B. Günther, A. Schwarzer, U. Böhme, *Z. Anorg. Allg. Chem.* **2014**, *640*, 1607–1613.
[44] U. Herzog: *Organosilicon halides – synthesis and properties, in The chemistry of organic silicon compounds* (Eds. Z. Rappoport, Y Apeloig), J. Wiley & Sons, Chichester, **2001**, Vol. 3, 469–489.
[45] Evonik press release from August 18th, 2001: Bau einer Spezialchemie-Anlage für Elektronikchips gestartet; https://corporate.evonik.de/de/unternehmen/ standorte/europa/deutschland/rheinfelden/Pages/article.aspx?articleId = 105329, accessed at November 11th, 2019.
[46] C. Bauch, S. Holl, R. Deltschew, S.-J. Mohsseni-Ala, G. Lippold, R. Towara, Verfahren und Vorrichtung zur Herstellung von kurzkettigen halogenierten Polysilanen, DE 10 2009 056 437 B4.
[47] C. J. Wilkins, *J. Chem. Soc.* **1953**, 3409–3412.
[48] A. Kaczmarczyk, G. Urry, *J. Am. Chem. Soc.* **1960**, *82*, 751–752.
[49] G. Urry, *Acc. Chem. Res.* **1970**, *3*, 306–312.
[50] S.-B. Choi, B.-K. Kim, P. Boudjouk, D. G. Grier, *J. Am. Chem. Soc.* **2001**, *123*, 8117–8118.
[51] J. Tillmann, F. Meyer-Wegner, A. Nadj, J. Becker-Baldus, T. Sinke, M. Bolte, M. C. Holthausen, M. Wagner, H.-W. Lerner, *Inorg. Chem.* **2012**, *51*, 8599–8606.
[52] J. I. Schweizer, L. Meyer, A. Nadj, M. Diefenbach, M. C. Holthausen, *Chem. Eur. J.* **2016**, *22*, 14328–14335.
[53] I. Georg, J. Teichmann, M. Bursch, J. Tillmann, B. Endeward, M. Bolte, H.-W. Lerner, S. Grimme, M. Wagner, *J. Am. Chem. Soc.* **2018**, *140*, 9696–9708.
[54] A. G. Sturm, J. I. Schweizer, L. Meyer, T. Santowski, N. Auner, M. C. Holthausen, *Chem. Eur. J.* **2018**, *24*, 17796–17801.
[55] F. Neumeyer, J. I. Schweizer, L. Meyer, A. G. Sturm, A. Nadj, M. C. Holthausen, N. Auner, *Chem. Eur. J.* **2017**, *23*, 12399–12405.
[56] F. Meyer-Wegner, A. Nadj, M. Bolte, N. Auner, M. Wagner, M. C. Holthausen, H.-W. Lerner, *Chem. Eur. J.* **2011**, *17*, 4715–4719.
[57] J. Teichmann, C. Kunkel, I. Georg, M. Moxter, T. Santowski, M. Bolte, H.-W. Lerner, S. Bade, M. Wagner, *Chem. Eur. J.* **2019**, *25*, 2740–2744.
[58] J. Tillmann, L. Meyer, J. I. Schweizer, M. Bolte, H.-W. Lerner, M. Wagner, M. C. Holthausen, *Chem. Eur. J.* **2014**, *20*, 9234–9239.
[59] M. Gerwig: Flüssige Hydridosilane als Precursoren zur Siliciumabscheidung, Ph. D. Thesis, Freiberg **2020**.
[60] F. Gründler, Synthese von perchlorierten Cyclohexasilanen durch chloridgesteuerte Disproportionierung von Hexachlordisilan: Eigenschaften und Reaktionsparameter, Bachelor Thesis, Freiberg, **2015**.
[61] D. K. Fleming, *Acta Crystallogr. Sect. B* **1972**, *28*, 1233–1236.
[62] D. F. Shriver, M. A. Drezdon: *The Manipulation of Air-Sensitive Compounds*, J. Wiley & Sons, New York, **1986**.
[63] U. Böhme: *Inertgastechnik*, Walter de Gruyter, Berlin, **2020**.
[64] https://www.hilgenberg-gmbh.de/en/innovative-glass-products/.
[65] M. Atoji, W. N. Lipscomb, P. I. Wheatley, *J. Chem. Phys.* **1955**, *23*, 1176–1176.
[66] H. W. Smith, W. N. Lipscomb, *J. Chem. Phys.* **1965**, *43*, 1060–1064.
[67] D. Brodalla, D. Mootz, R. Boese, W. Osswald, *J. Appl. Crystallogr.* **1985**, *18*, 316–319.
[68] R. Boese, M. Nussbaumer: In situ Crystallization Techniques, in *Correlations, Transformations, and Interactions in Organic Crystal Chemistry, IUCr Crystallographic Symposia* Vol. 7, (Eds. D. W. Jones and A. Katrusiak) Oxford University Press, Oxford, England, **1994**, pp. 20–37.
[69] R. Boese, H. C. Weiss, D. Bläser, *Angew. Chem. Int. Ed.* **1999**, *38*, 988–992. *Angew. Chem.* **1999**, *111*, 1042–1045.
[70] R. Boese, M. Yu. Antipin, M. Nussbaumer, D. Bläser, *Liq. Cryst.* **1992**, *12*, 431–440.
[71] A. D. Bond, J. E. Davies, *Z. Kristallogr.* **2014**, *229*, 661–666.
[72] K. Merz, R. Bieda, *Z. Kristallogr.* **2014**, *229*, 635–638.
[73] R. Boese, *Z. Kristallogr.* **2014**, *229*, 595–601.
[74] F. Fehér, R. Freund, *Inorg. Nucl. Chem. Lett.* **1973**, *9*, 937–940.
[75] E. Hengge, D. Kovar, *Z. Anorg. Allg. Chem.* **1979**, *459*, 123–130.
[76] J. R. Dahn, B. M. Way, E. Fuller, J. S. Tse, *Phys. Rev. B* **1993**, *48*, 17872–17877.
[77] O. Degtyareva, M. M. Canales, A. Bergara, X.-J. Chen, Y. Song, V. V. Struzhkin, H.-K. Mao, R. J. Hemley, *Phys. Rev. B* **2007**, *76*, 064123.
[78] Y. Li, G. Gao, Q. Li, Y. Ma, G. Zou, *Phys. Rev. B* **2010**, *82*, 064104.
[79] M. J. Barrow, E. A. V. Ebsworth, M. M. Harding, *Acta Crystallogr. Sect. B* **1979**, *35*, 2093–2099.
[80] G. Becker, B. Eschbach, D. Käshammer, O. Mundt, *Z. Anorg. Allg. Chem.* **1994**, *620*, 29–40.
[81] M. J. Barrow, E. A. V. Ebsworth, *J. Chem. Soc. Dalton Trans.* **1984**, 563–565.
[82] B. Beagley, A. R. Conrad, J. M. Freeman, J. J. Monaghan, B. G. Norton, G. C. Holywell, *J. Mol. Struct.* **1972**, *11*, 371–380.
[83] A. Haaland, K. Rypdal, H. Stüger, H. V. Volden, *Acta Chem. Scand.* **1994**, *48*, 46–51.
[84] Z. Smith, H. M. Seip, E. Hengge, G. Bauer, *Acta Chem. Scand.*, **1976**, *A30*, 697–702.
[85] Z. Smith, A. Almenningen, E. Hengge, D. Kovar, *J. Am. Chem. Soc.* **1982**, *104*, 4362–4366.
[86] A. Bondi, *J. Phys. Chem.* **1964**, *68*, 441–451.
[87] S. Alvarez, *Dalton Trans.* **2013**, *42*, 8617–8636.
[88] A. Gavezzotti: Molecular Aggreagation, Oxford University Press, Oxford **2013**, p. 203.
[89] A. I. Kitajgorodskij: *Molecular Crystals and Molecules*, New-York, Academic Press, **1973**.
[90] N. Wiberg: *Hollemann, Wiberg – Lehrbuch der Anorganischen Chemie*, de Gruyter, 102. Auflage, Berlin **2007**, p. 117.
[91] R. Kahn, R. Fourme, D. Andre, M. Renaud, *Acta Crystallogr. Sect. B* **1973**, *29*, 131–138.
[92] A. Torrisi, C. K. Leech, K. Shankland, W. I. F. David, R. M. Ibberson, J. Benet-Buchholz, R. Boese, M. Leslie, C. R. A. Catlow, S. L. Price, *J. Phys. Chem.* **2008**, *B112*, 3746–3758.
[93] V. R. Thalladi, R. Boese, *New J. Chem.* **2000**, *24*, 579–581.
[94] Handbook of Stable Isotope Analytical Techniques, P. A. de Groot (Ed.), Elsevier, Amsterdam, 2009, Vol. 2, 619–619.
[95] C. Chatgilialoglu, *Chem. Rev.* **1995**, *95*, 1229–1251.
[96] A. J. McKinley, T. Karatsu, G. M. Wallraff, D. P. Thompson, R. D. Miller, J. Michl, *J. Am. Chem. Soc.* **1991**, *113*, 2003–2010.
[97] S. Inoue, M. Ichinohe, A. Sekiguchi, *J. Am. Chem. Soc.* **2007**, *129*, 6096–6097.
[98] C. Chatgilialoglu, C. H. Schiesser in *The chemistry of functional groups* (Eds.: Y. Apeloig, S. Patai, Z. Rappoport), John Wiley & Sons, Ltd, Chichester, **1989**, pp. 341–390.
[99] J. Tillmann, H.-W. Lerner, M. Bolte, *Acta Crystallogr. Sect. E* **2020**, *76*, 261–263.
[100] Stoe & Cie (**2009**). X-RED and X-AREA. Stoe & Cie, Darmstadt, Germany.
[101] G. M. Sheldrick, *Acta Crystallogr. Sect. A* **2008**, *64*, 112–122.
[102] G. M. Sheldrick, *Acta Crystallogr. Sect. C* **2015**, *71*, 3–8.

Manuscript received: May 27, 2020
Revised manuscript received: June 4, 2020